



VLC
4607



Wairakei Research Centre
114 Karetoto Road
Wairakei, Taupo 3377
Private Bag 2000
Taupo 3352
New Zealand
T +64-7-374 8211
F +64-7-374 8199
www.gns.cri.nz

**Magma ascent during eruptions at
Mt. Ngauruhoe: insights from xenolith
fluid inclusions**

G. Kilgour
F. Della Pasqua
G. Jolly

**GNS Science Consultancy Report 2009/168
June 2009**

DISCLAIMER

This report has been prepared by the Institute of Geological and Nuclear Sciences Limited (GNS Science) exclusively for and under contract to EQC. Unless otherwise agreed in writing by GNS Science, GNS Science accepts no responsibility for any use of, or reliance on any contents of this Report by any person other than EQC and shall not be liable to any person other than EQC, on any ground, for any loss, damage or expense arising from such use or reliance.

BIBLIOGRAPHIC REFERENCE

Kilgour, G.; Della Pasqua, F.; Jolly, G. 2009. Magma ascent during eruptions at Mt. Ngauruhoe: insights from xenolith fluid inclusions, *GNS Science Consultancy Report 2009/168*. 20p.

CONTENTS

EXECUTIVE SUMMARY	ii
INTRODUCTION.....	1
DETERMINING THE DEPTH OF ORIGIN FOR THE XENOLITHS	2
Methods	2
Laser Raman spectroscopy.....	3
Microthermometry - fluid inclusion stage	3
Background information on fluid inclusions	4
Results	4
CO ₂ content of xenolith inclusions	4
Depth of origin of xenoliths	6
ASCENT RATE OF NGAURUHOE MAGMA	7
Methods	7
Density measurements of xenoliths.....	7
Chemical composition of the lava	7
Water content of the volcanic glass	7
Results	8
Density measurements of xenoliths.....	8
Water content of volcanic glass	8
Viscosity of Ngauruhoe magma.....	9
DISCUSSION.....	10
Pressure of CO ₂ fluid entrapment and implications for magma storage depth	10
Ascent rates of magma from density calculations	12
CONCLUSIONS.....	14
REFERENCES.....	15
ACKNOWLEDGEMENTS	16

FIGURES

Figure 1	Location map of Ngauruhoe volcano within the Taupo Volcanic Zone.	1
Figure 2	Field photo of a quartz-rich xenolith from the 1975 eruption of Ngauruhoe.	2
Figure 3	Laboratory photos of the Laser Raman	3
Figure 4	Schematic representation showing the formation of primary and secondary inclusions during and post crystal growth.	4
Figure 5	Thin section photomicrographs of various types of xenolithic quartz crystals and some inclusions within them.	5
Figure 6	Phase transition photomicrographs of a fluid inclusion in sample 23A-2B showing a sequence of phase transitions during a freezing/heating experiment.	6
Figure 7	Graph showing the effect that small changes in either H ₂ O and/or temperature have on the viscosity.	9
Figure 8	Calculated pressure ranges for trapped fluids in the Ngauruhoe inclusions.	12
Figure 9	Schematic diagram of the sub-surface magmatic plumbing system ofr Ngauruhoe.	14

TABLES

Table 1	Laser Raman results from fluid inclusions.	7
Table 2	Density values for quartzite xenoliths from the 1975 eruption of Ngauruhoe.	8
Table 3	H ₂ O water content determined by Laser Raman spectroscopy on volcanic glass.	10

EXECUTIVE SUMMARY

We have completed a petrological study on the scoria from the 1975 eruption of Ngauruhoe volcano. We analysed a number of quartz-rich xenoliths and the fluid inclusions that were trapped within them. The fluid inclusions that were composed of CO₂ revealed that their trapping pressures were very tightly grouped. Both primary and secondary inclusions recorded a trapping pressure equivalent to 1.5 – 3.5 km depth. It is likely that a series of shallow magma chambers were occupied at this depth prior to the 1975 eruption and probably remain at present.

The density of the xenoliths relative to the magma provided us with a method to calculate the minimum ascent rate for the magma. A rate of 1.0 mh⁻¹ suggests that the travel time from the xenolith origin (magma chamber depth) to the surface is approximately 2 – 4 months. Therefore any future activity that exhibits low-frequency earthquakes may provide a significant warning to future magmatic eruptions at Ngauruhoe. This petrological study will aid in the interpretation of future seismic crises and may help to constrain the depths at which these events are sourced.

INTRODUCTION

Mount Ngauruhoe is a frequently active andesite to basaltic-andesite volcano (Figure 1) located in the southern part of the Taupo Volcanic Zone. Eruptions from Ngauruhoe have ranged from explosive to effusive episodes over very short time intervals. Eye witness accounts of historic eruptions from Ngauruhoe are well-documented, but the reason behind a change in the style of eruptions is poorly understood. Seismic precursors to historic eruptions at Ngauruhoe are not well documented, but a swarm of long period earthquakes has been ongoing since 2006. Although thought at first to signal a return to a more active period, no surface activity (e.g. magmatic eruption or changes in fumarolic and/or soil gas composition and temperatures) has been detected by GeoNet. Clearly, we need to understand how magma is generated and then rises to the surface prior to eruption.

In order to examine the dynamics of the magma chamber and conduit system from depth to surface, we proposed to use one conspicuous aspect of the eruptive products from Ngauruhoe: the ubiquitous presence of quartz-rich accidental rock fragments or xenoliths (Figure 2) in the 1975 magma. A number of studies have examined the origin of these fragments (Steiner, 1958; Graham, 1987; Graham et al., 1988; Hobden, 1997), and their original rock type has been debated, but an estimate of the depth of origin has been largely overlooked (c.f. Graham et al., 1988). In this study we aimed to determine the depth of origin of these xenoliths using the information retained in CO₂-rich inclusions within quartz crystals. We then envisaged that we could determine the settling velocity of these ubiquitous xenoliths within the Ngauruhoe magma and calculate the minimum ascent velocity for the magma prior to eruption.

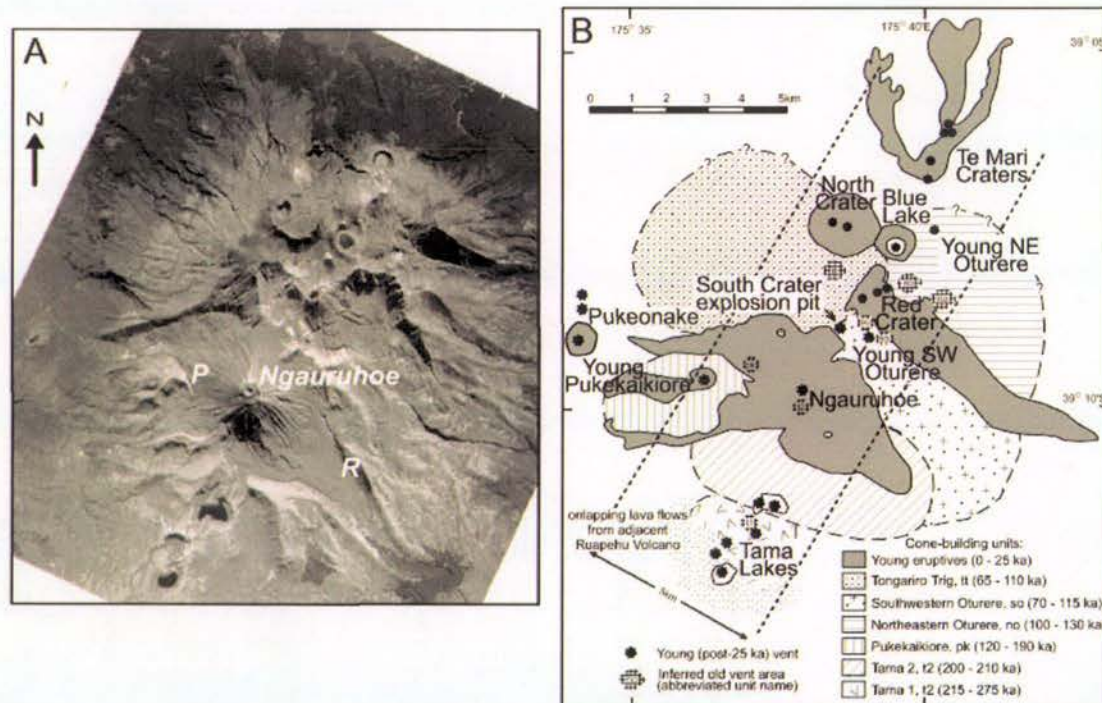


Figure 1 Aerial photograph (A) and location map of Ngauruhoe associated with other cones in the Tongariro Volcanic Centre from Hobden et al. (2002). P is Pukekaikio and R is the Waihohonu Valley Ridge.



Figure 2 Field photo showing a sharp-edged, quartz-rich xenolith (light coloured) within a strongly agglutinated (welded) scoria deposit from the 1975 eruption of Ngauruhoe.

Our study has focussed on the products of the 1974-1975 explosive eruption of Ngauruhoe (e.g. Nairn, 1976; Nairn & Self, 1978; Self et al., 1979). By confining our study to this event, we hoped to examine trends (if any) in the depths of xenoliths through the eruption sequence, and especially to test whether primary and secondary fluid inclusions were developed under different pressures (and hence depth). This study has been used as a test of the various techniques employed and, if successful, we intend to determine the original depth of xenoliths throughout the Tongariro Volcanic Centre (including Ruapehu) to see if there are differences in depths of magma generation and storage across the massif.

Unfortunately, seismic monitoring during the 1975 eruptions at Ngauruhoe was inadequate to determine the depth of seismicity before eruptions, so we cannot compare our results directly with the historic data. However, a next stage of the project will be to assess our conceptual model of the plumbing system in the light of ongoing finite difference modelling of the recent long period seismicity (A Jolly pers. comm.).

DETERMINING THE DEPTH OF ORIGIN FOR THE XENOLITHS

Methods

Two laboratory procedures were used to analyse the fluid inclusions within quartz crystals of xenoliths from the 1975 eruption of Ngauruhoe volcano, so that we could determine where the xenoliths were incorporated into the magma. In order to determine the trapping pressures and hence the depth of origin of the xenoliths, first we needed to ascertain whether CO₂-rich inclusions are present (Laser Raman spectroscopy) and then determine their respective homogenisation temperatures (heated stage microscopy).

Laser Raman spectroscopy

We made 4 polished thick sections (c. 100 μm) of selected xenoliths and found a number of fluid inclusions within quartz crystals for analysis by Laser Raman spectroscopy at Geoscience Australia, Canberra (Figure 3). Laser Raman spectroscopy is a technique that can analyse the composition of fluid or gas species trapped in small inclusions. The technique uses a modified optical microscope, where a laser beam is focussed through the microscope objectives (ca. 1 μm across), through the sample and analysed via a receiver, producing a spectrogram. Raman spectra were recorded on a Microdil-28 Raman microprobe (Liu and Mernagh, 1990). The 514.5 nm line from a Spectra Physics 2020 argon ion laser was used as the excitation source. Determining the gas species is achieved by matching the spectra peaks with known standards. The relative proportions of the gases are calculated from known quantification constants. The behaviour of these inclusions during heating/freezing experiments was then examined, using the fluid inclusion microthermometry stage at Wairakei Research Centre – GNS Science.

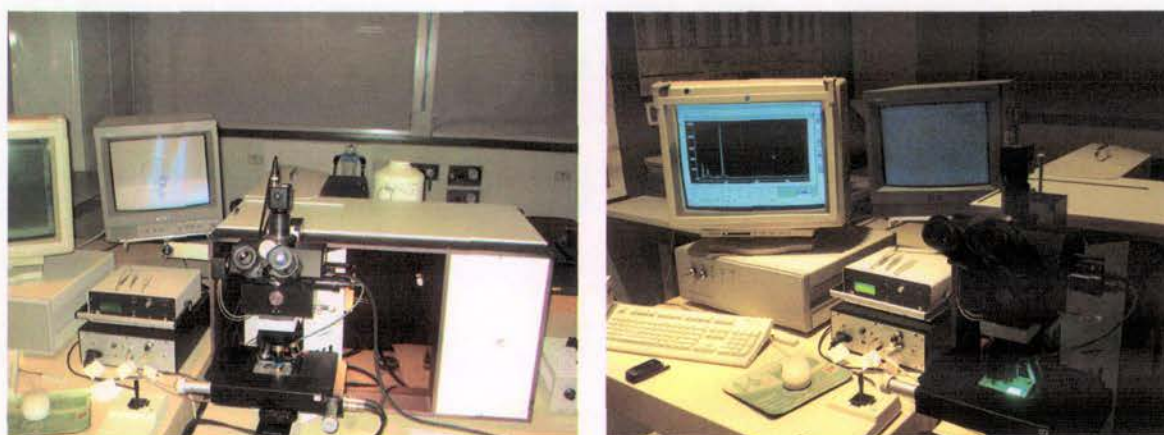


Figure 3 The Laser Raman is a non-destructive technique that passes a laser beam through the inclusion using a modified optical microscope (left). After positioning the laser onto the desired inclusion (beam size of ca. 1 μm), a Raman spectra (right) is produced. In this case, a significant CO_2 peak is evident.

Microthermometry - fluid inclusion stage

Fluid inclusion microthermometry heating and freezing experiments were carried out on 4 Ngauruhoe quartzite xenoliths, using a Linkam THMSG600 heating and cooling stage, which is controlled by Linksys 32 DV software, housed at GNS Science, Wairakei. Based on the results from the Laser Raman, we were able to restrict our analyses to CO_2 -rich inclusions. Freezing of an inclusion to c. $-60\text{ }^\circ\text{C}$ reaffirmed the presence of CO_2 in the inclusions and consequently heating measurements were then conducted. Heating until the vapour in the inclusion homogenises, gives the T_h (homogenisation temperature of the vapour), which is then used to determine the density of the fluid trapped in the inclusion and hence the pressure at which the vapour was trapped within the quartz crystal (e.g. Zanon et al., 2003). Most of the inclusions analysed are considered primary and therefore are probably related to initial quartz growth.

Background information on fluid inclusions

When a crystal grows in the presence of a fluid phase, some of the fluid may be trapped within imperfections of the growing crystal to form fluid inclusions (Bodnar, 2003). The classification of fluid inclusions are most commonly related to timing of inclusion formation relative to crystal growth. As such, primary fluid inclusions are formed during growth of the host crystal. If a crystal fractures after it has formed, some fluid may become trapped as secondary fluid inclusions when the fracture heals (Figure 4). In practice, classifying fluid inclusions into either primary or secondary groupings is often complex. In the case of the 1975 Ngauruhoe quartzite xenoliths, we have assumed that the growth of the xenolith has occurred in a concentric fashion. Therefore, all inclusions that appear to conform to a concentric pattern are here regarded as primary, while those inclusions that appear to form as a lineament/s perpendicular or sub-perpendicular to the general crystal growth pattern are here regarded as secondary.

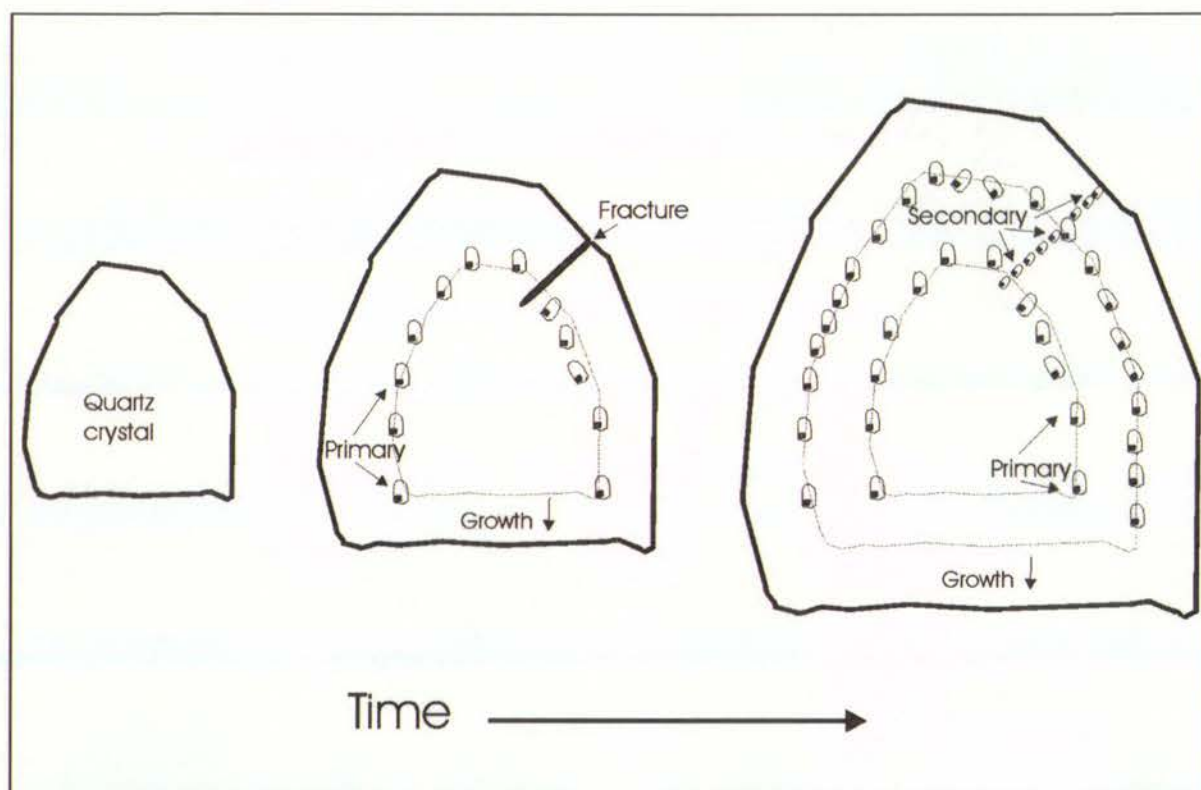


Figure 4 Schematic representation showing the formation of primary and secondary inclusions during and post crystal growth.

Results

CO₂ content of xenolith inclusions

Of the 4 xenolith thick sections that were analysed by Laser Raman spectroscopy, a total of 54 inclusions were examined, leading to 140 individual spectra. The total number of analyses included both the fluid and gas phases of many inclusions (Figures 5 and 6). From the 140 spectra, only 8 spectra from separate inclusions contained suitable information for this study (Table 1). The vast majority of the primary inclusions were dry and contained no trace of either H₂O or CO₂.

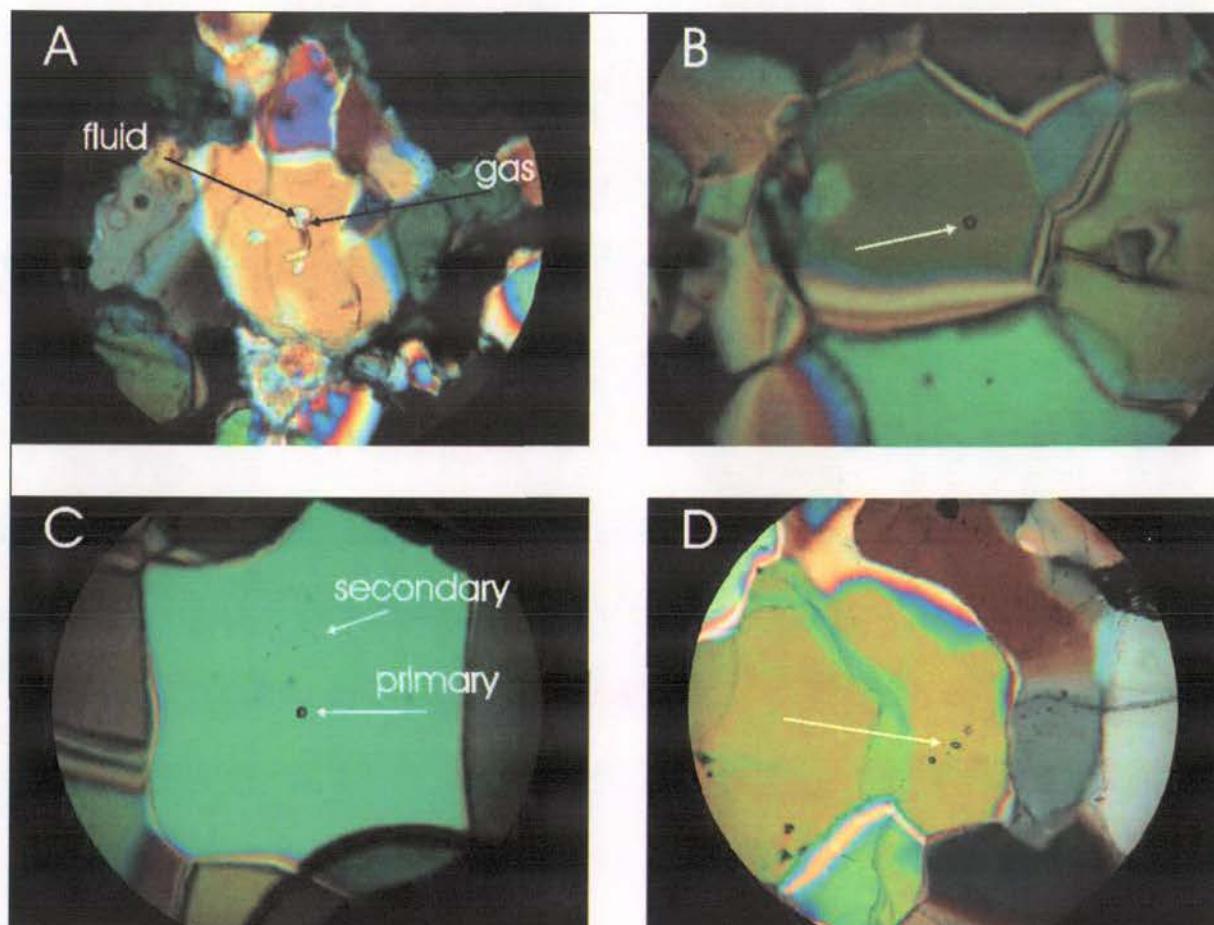


Figure 5 Thin section photomicrographs of xenolithic quartz crystals and some inclusions within them. (A) Primary fluid inclusion with a gas bubble and liquid phase (XF3-1). (B) Primary fluid inclusion near the centre of a quartz crystal (XG4a-1). (C) Quartz crystal with both primary and secondary inclusions (XG8a-1). (D) A trail of secondary inclusions that cut across the original quartz growth pattern. Magnification in photos B, C, and D are 20x, while the magnification in A is 5x (23A2B/C). Arrow in (D) points to inclusion in Figure 6.

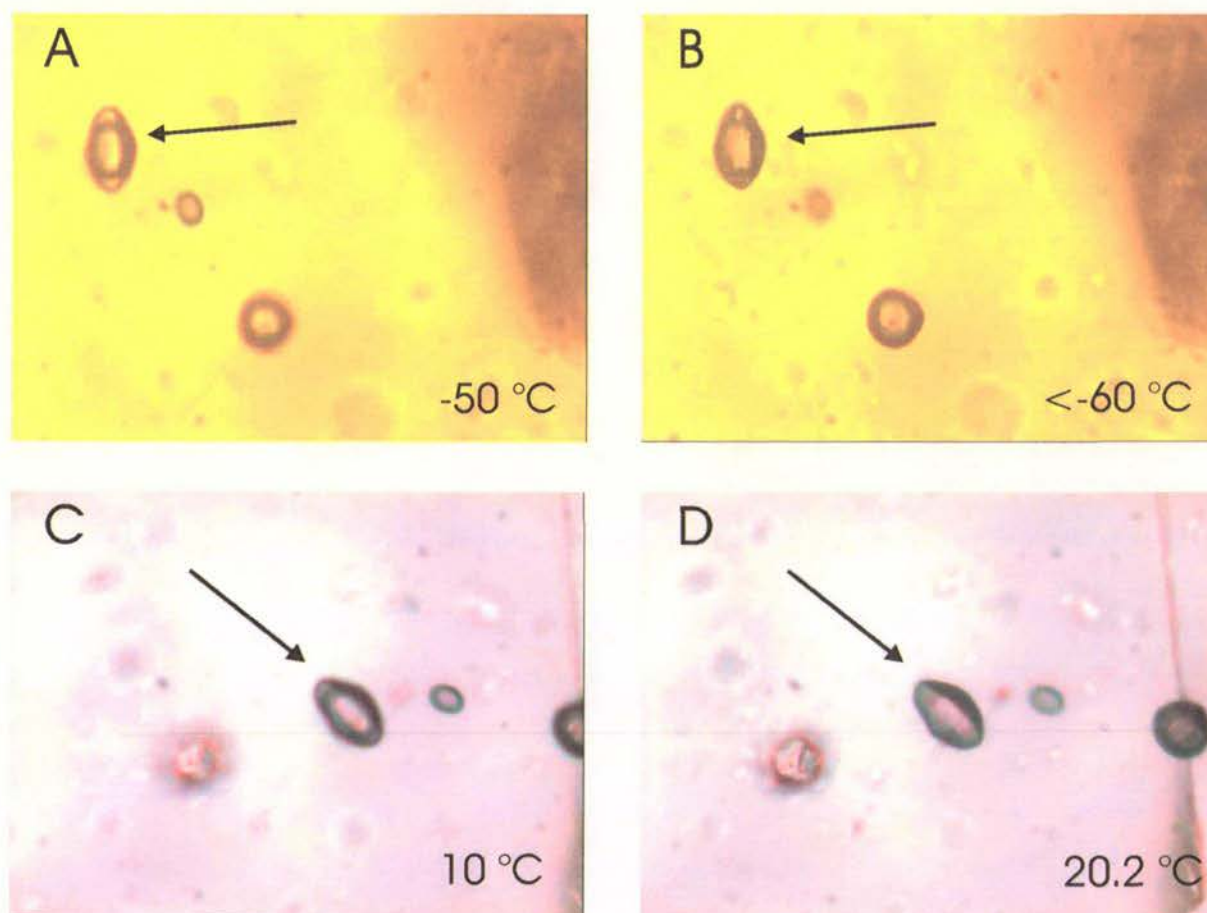


Figure 6 Phase transition photomicrographs of a fluid inclusion in sample 23A-2B showing a sequence of phase transitions during a freezing/heating experiment. (A) Vapour rich, secondary inclusion exhibits a clear bubble at $-50\text{ }^{\circ}\text{C}$. (B) Bubble has completely frozen beyond $-60\text{ }^{\circ}\text{C}$. (C) Again the inclusion exhibits a clear bubble at $10\text{ }^{\circ}\text{C}$. (D) During heating to $20.2\text{ }^{\circ}\text{C}$, the vapour homogenizes and the bubble expands to its limits. Arrow points to the same inclusion in all photos. Magnification in all photos is 40x.

Depth of origin of xenoliths

The density of the vapour in the inclusions found in xenocrystic quartz, as determined by the microthermometry experiments, has given us an estimate of the depth at which the quartz-rich xenoliths originate. The range in density values for the inclusions is tightly clustered (Table 1). This apparent clustering of densities may be an artefact of the small number of analyses and it is possible that a more comprehensive study could determine whether our sample size is representative. However, we have shown that the technique can be employed on xenoliths from a cone volcano, and thus will likely be applicable to xenoliths obtained from other cone volcanoes in New Zealand.

Table 1 Laser Raman results from fluid inclusions found in quartzite xenoliths from the 1975 eruption of Ngauruhoe. Density and depth calculations for each inclusion are also included. Sample numbers in bold indicate primary fluid inclusions. All others are secondary.

Sample Number	CO ₂ mol %	N ₂ mol %	Freezing Temp (°C)	Homogenisation Temp Th _v (°C)	Density of fluid in Inclusion (g/cm ³)	Pressure (GPa)	Depth (km)
23A2B-3	100	0	-58.9	20.2	0.1954	0.0571	2.3
23A2C-3	100	0	-59.1	20.5	0.1989	0.0581	2.3
XF3-1	86	14	-59.3	24.0	0.2479	0.0724	2.9
XG4a-1	93	7	-58.8	27.4	0.3096	0.0904	3.6
XG8a-1	82	18	-59.6	10.0	0.1401	0.0409	1.6
XG4b	100	0	-59.1	18.7	0.1794	0.0524	2.1
XG4c	100	0	-58.8	20.5	0.1989	0.0581	2.3
XG4d	100	0	-59.1	23.0	0.2324	0.0679	2.7

ASCENT RATE OF NGAURUHOE MAGMA

The second question that we are trying to answer is how fast the magma travels to the surface. In order to determine this parameter, we need to employ Stokes' Law to calculate the minimum settling velocity of the xenoliths in the magma. Thus we need to measure or calculate some key properties of the xenoliths (density) and the magma (viscosity).

Methods

Density measurements of xenoliths

In order to measure the relative density of the xenoliths within the magma, we employed the density method of Carmichael (1984). This method is simple and requires little sample preparation. Essentially the xenoliths were cleaned of all volcanic glass and scoria from the margins and heated to 110 °C for at least 24 hours and then weighed (dry weight). The samples were also weighed in water, as well as under vacuum and in water. Using the simple calculations of Carmichael (1984), we have calculated the density for 15 xenoliths (Table 2).

Chemical composition of the lava

We used the geochemical composition of the basaltic andesite from the 1975 Ngauruhoe eruption from Hobden (1997). That work involved a detailed study of the geochemical history of Ngauruhoe and so we did not deem it necessary to repeat that work. Hobden's geochemical data was used to calculate the viscosity of the magma, which was vital for ascent rate calculation.

Water content of the volcanic glass

A key component for the calculation of viscosity of magmas is the magmatic water content. Many studies have shown that small increases in water content can have significant effects on the viscosity of a magma (e.g. Shaw, 1972; Giordano & Dingwell, 2003; Hui & Zhang, 2007; Giordano et al., 2008). Two laboratory methods were employed to measure the water content of the Ngauruhoe magma. Firstly, Laser Raman spectroscopy of the volcanic glass

was used. During our Laser Raman analysis of the volcanic glass at GeoScience Australia, it became apparent that the abundance of microlites would cause problems with the analysis, since there was little microlite free clear glass visible in the samples. However, there were some areas of the scoria that were microlite-poor and measurements were conducted in these areas of the rock.

A secondary method for determining water content was to use the loss on ignition (LOI) while conducting X-ray Fluorescence (XRF) analysis. Although not ideal, this method gives an approximation of the water driven out of the bulk rock (during heating of the sample to c. 600 °C). Here we used data from Hobden (1997).

Results

Density measurements of xenoliths

The densities of the xenoliths are uniform through most of the 16 samples analysed. All of the quartzite xenoliths exhibit a wet density of ca. 2.5 g/cm³ (Table 2). A small number of outlier densities are significantly lower, 1.84 – 2.01 g/cm³, probably caused by the weak and fractured nature of these 4 samples.

Table 2 Density values for quartzite xenoliths from the 1975 eruption of Ngauruhoe.

Sample	Dry Density g/cm ³	Wet Density (Saturated) g/cm ³
NG27a	2.40	2.49
NG27b	2.41	2.49
NG27c	2.35	2.49
NG27d	2.44	2.52
NG27e	2.40	2.49
NG27f	2.31	2.42
NG27g	2.47	2.54
NG27h	2.32	2.43
NG27i	2.47	2.54
NG23	2.31	2.42
NG18	1.64	1.95
NG21	2.50	2.55
NG28	2.41	2.50
NG10	1.44	1.89
NG15	1.62	2.01
NG11	1.38	1.84

Water content of volcanic glass

When analysing the volcanic glass to determine the water content of the magma, the Laser Raman spectroscopy results show that the magma is water-poor (< 2%) although the results are less than ideal. Due to the iron-rich nature of the volcanic glass, significant fluorescence of the laser resulted in disparate results when using different water calculations (Table 3). Hence these results are variable.

LOI results from the XRF analyses also showed that the magma is water-poor and values of < 2 % were common and in some cases were less than 1 %. These differing techniques confirm the water content for the magma to be c. 1 % (Table 3).

In addition, we examined the Ngauruhoe scoria and lava in thin section and observed that the mineralogy of the lava was anhydrous (water-free) due to the absence of water-bearing minerals such as amphibole. In similar studies overseas (e.g. Giordano & Dingwell, 2003; Hui & Zhang, 2007; Giordano et al., 2008), these amphibole-free magmas generally contain less than 2 % water and, in most cases, are essentially dry (< 1 % water).

Viscosity of Ngauruhoe magma

The viscosity of the 1975 basaltic-andesite magma has been calculated from the model of Giordano et al. (2008). Their formula for calculating viscosity is:

$$\text{Log } \eta = \frac{A + B}{\text{Temp}(K) - C} \text{ Pa s} \quad (1)$$

where A is a constant (-4.55) representing an upper temperature limit for viscosity, B and C represent the geochemical composition of the magma including water content, and Temp(K) is the temperature of the magma in Kelvin (in this case we used a range from 1100 to 1500 °K). In the equation above, B and C refer to 13 major oxide compositions, which were obtained through XRF analysis.

As shown in Figure 7, small variations in either temperature or water content can significantly affect the calculated viscosity. Therefore the calculations above, have an error of $\pm 20 - 40$ %. We assumed a magmatic temperature of 1100 °C or 1373 °K, based on Hobden's (1997) geothermometry.

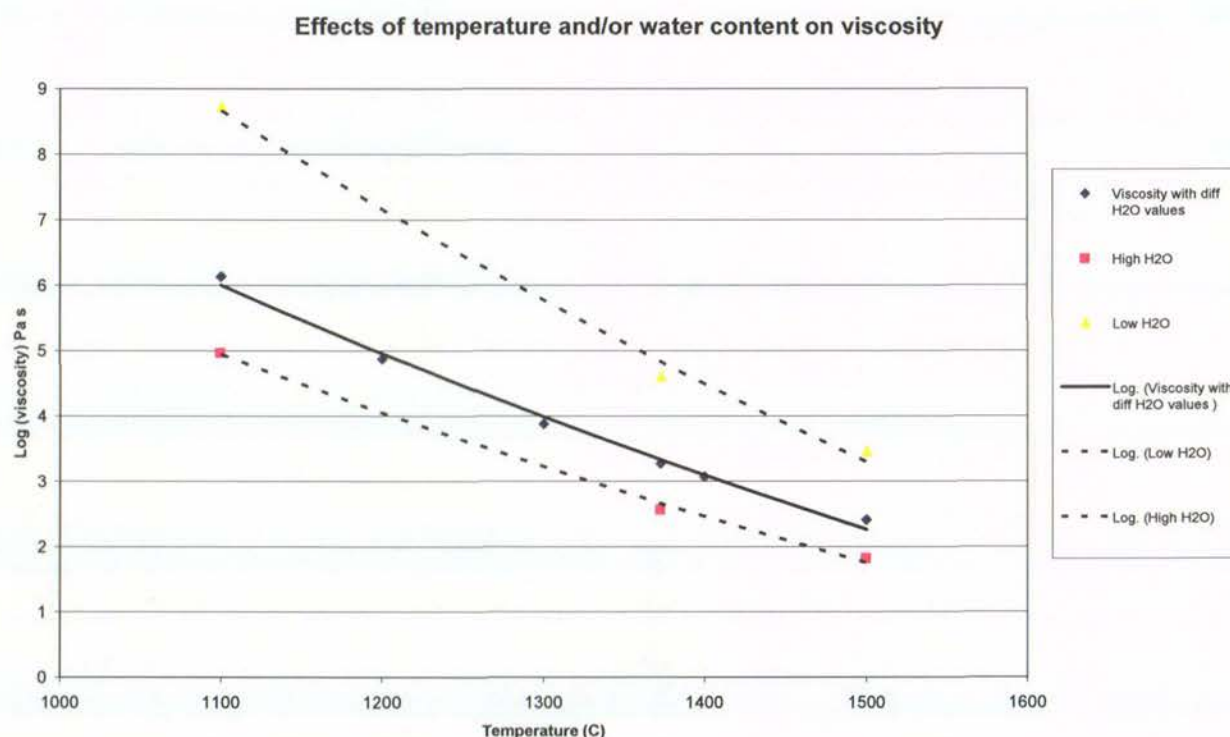


Figure 7 Graph showing the effect that small changes in either H₂O and/or temperature have on the viscosity. The blue line represents the viscosity of a magma that contains 1 % by weight H₂O over a range of temperatures. We assumed a temperature of 1373 K for the calculations in the text. The red and green lines represent the viscosity of a magma with 0 and 2.5 % H₂O respectively.

Table 3 H₂O water content determined by Laser Raman spectroscopy on volcanic glass. The intensity and integral numbers refer to the Raman spectra over which the water content is determined. The method used to calculate the water content uses the intensity ratio method, outlined in Di Muro et al. (2008)

Sample No.	Intensity 3550 cm ⁻¹	Integral 3100 – 3750 cm ⁻¹	Intensity <490 cm ⁻¹	Integral 490 cm ⁻¹	H ₂ O _T /TOT (Intensity ratio)	Calc H ₂ O _T (wt%)
13A11A	11	98971	6307	212517	0.00169	0.36
13A11B	98	6435	2883	126533	0.03413	0.68
13AS6	1007	336453	9521	588173	0.10581	1.38
8Bii1b	321	151127	1945	565904	0.16496	1.97
8Bii2b	36	23415	882	54433	0.04053	0.74
XD2	9	8134	63404	1239967	0.00015	0.34
XF1	546	188853	15589	692340	0.03505	0.68
XF2	872	634527	7918	391003	0.11014	1.43
XF3	403	116162	38234	628539	0.01055	0.44
XF5	175	111059	14455	224190	0.01211	0.46
XF6	1287	341861	56473	1284999	0.02279	0.56
XF7a	72	27523	32729	506933	0.00221	0.36
XF7b	127	94069	41983	727932	0.00303	0.37
XF7c	2	5629	30020	382635	0.00007	0.34
XF7d	11	5887	61448	823907	0.00018	0.34
XF7e	22	4773	22985	306669	0.00098	0.35
XG3c	411	133972	12235	285919	0.03361	0.67
XG3d	212	64293	16609	322570	0.01278	0.46
XG4a	434	358280	12215	202993	0.03551	0.69
XG7a	16	3626	15666	249951	0.00099	0.35
XG7c	24	21113	63782	999023	0.00038	0.34
XG8a	1	10230	63542	1150924	0.00002	0.34
XG8b	45	31030	37937	591068	0.00120	0.35

DISCUSSION

Pressure of CO₂ fluid entrapment and implications for magma storage depth

The analysis of the vapour/fluid composition and density of fluid inclusions within quartzite xenoliths has resulted in an assessment of the trapping pressures and temperatures for the CO₂, and therefore a range for the depth at which the xenoliths originated or resided before eruption. The inclusions analysed include both primary and secondary inclusions and are likely to indicate the depth at which the xenoliths resided before eruption (and potentially in contact with a magma chamber). This is an important consideration, as we had hypothesised that more than one population of trapping pressures in the inclusions may be present (i.e. primary inclusions exhibit high pressures and represent greater depths while secondary inclusions exhibit low pressures and shallow depths). We believe that we are able to show that the fluid inclusions analysed here record the depth at which xenoliths were incorporated

into the Ngauruhoe magma. Figure 8 shows the pressures calculated from the fluid inclusion analyses and the inferred depths. Although based on a limited number of CO₂-rich inclusions, a pattern has emerged. Inclusions analysed within this study give pressure estimates of 0.04 – 0.09 GPa at ca. 1100 °C (assumed from previous work – Hobden, 1997). These pressures correspond to depths of 1.6 – 3.6 km (here these depths refer to below mean sea level, as assumed in Zanon et al., 2003).

It has been proposed at other volcanoes that relatively low-density fluid inclusion peaks, similar to those found in this study, may reflect a period of xenolith residence within or in contact with shallow magma chambers (e.g., Vaggelli et al., 1993; Lima, 1996; Zanon et al., 2003). This is difficult to prove in this case, as we would be required to conduct this type of study for all Ngauruhoe eruptives in order to confirm whether a common shallow magma exists between ca. 1.5 and 3.5 km depth. Rowlands et al. (2005) showed through seismic tomography that a low velocity volume exists beneath the cone of Ngauruhoe from ca. 3 to 6 km depth. Graham et al. (1998) also concluded from experimental work that the xenoliths found in Ngauruhoe eruptives are derived from less than 5 km depth. The low velocity zone of Rowlands et al. (2005) may coincide with a complex network of shallow magma chambers inferred from detailed geochemistry work from Hobden et al. (1999). A network of magma chambers is consistent with our depth estimates of xenolith incorporation from the fluid inclusion results, which indicate the presence of a shallow magma reservoir (and possibly many reservoirs). Following Hobden et al. (1999), there are likely to be a number of small magma storage reservoirs, all with their own unique geochemical history. Such a network of chambers increases the likelihood of interaction with country rock leading to incorporation into the conduit and eventually to eruption as xenoliths (Figure 9). Shallow magma chambers are also consistent with recent long period seismicity, which is thought to be located at ca. 1 km depth to the north of the cone (S. Sherburn, pers. comm.).

Another possible explanation for the shallow xenolith entrainment is due to the force of shearing along the conduit walls. Del Gaudio & Ventura (2008) proposed a mechanism for xenolith entrainment via magma movement in a conduit rather than due to shallow magma residence. In their paper, they show that the forces of shearing, due to an increase in viscosity caused by crystallisation and cooling could erode the margins of the conduit, thereby enabling the xenoliths to be incorporated during magma transport. Del Gaudio & Ventura (2008) indicate that magma convection or simply stagnated magma reservoirs cannot adequately erode the country rock and be incorporated into the magma. Whichever model becomes more accepted is beyond the scope of this work, but it does provide alternative modes for xenolith incorporation.

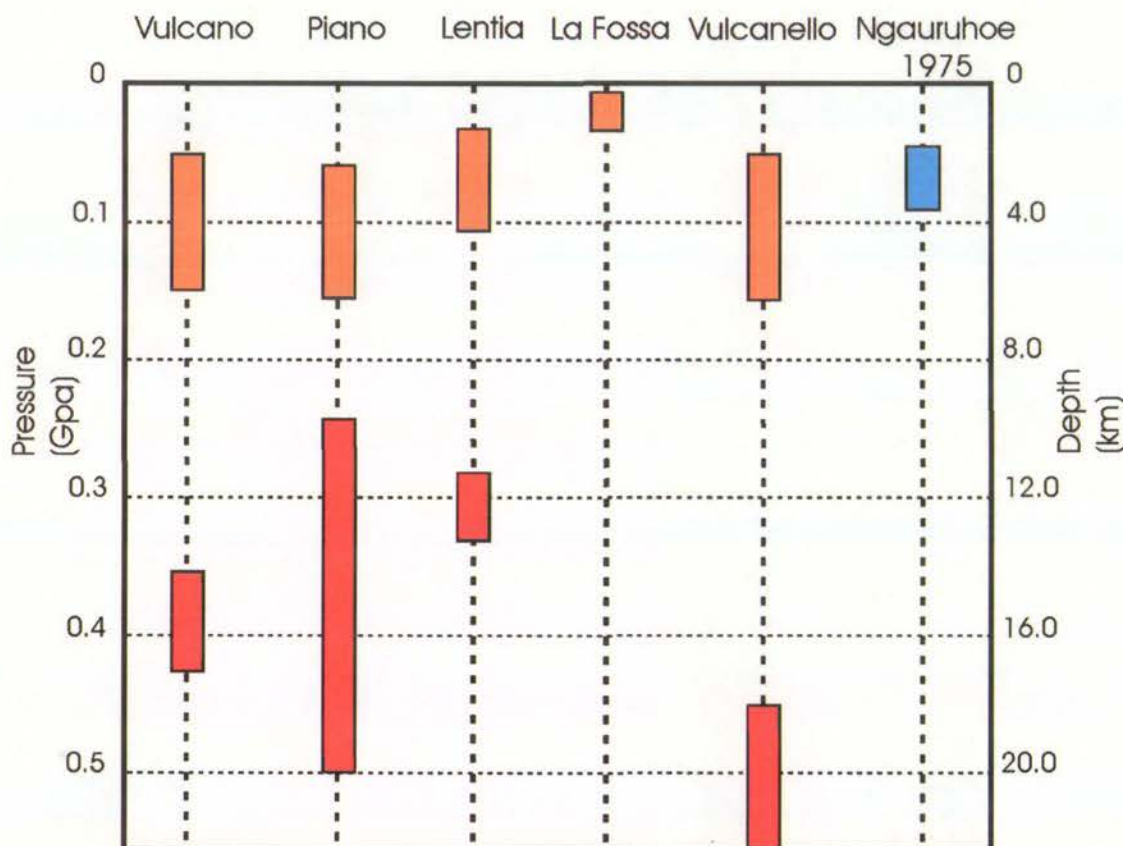


Figure 8 Calculated pressure ranges for trapped fluids in the Ngauruhoe inclusions with examples for comparison from Vulcano Island, Italy (Zanon et al., 2003; Clocchiatti et al., 1994). There appears to be only one trapping episode for these xenoliths. The shallow depth inferred from these inclusions indicates the presence of a shallow magma reservoir/s between 1.5 and 3.5 km depth.

Before the 1975 eruption of Ngauruhoe, Latter (1981) suggested that eruption earthquakes may occur from 0.2 to 1.5 km below the summit of the volcano, although precursory seismic activity was probably at a greater depth. Although a significant amount of error is likely to be inherent in these depth estimates due to limited seismic stations, it is possible that the pre-eruptive seismicity was recording the movement of magma within the conduit, originating from the shallow magma chamber/s that exists or existed between 1.5 and 3.5 km depth. For future magmatic events at Ngauruhoe we might expect to see seismicity originating at these depths.

Ascent rates of magma from density calculations

Estimating ascent rates of magma requires analyses of three main variables, being viscosity and both xenolith and magma densities. For this calculation, we used Stokes' settling velocity V :

$$V = \frac{2gr^2(P_x - P_m)}{9n} \quad (2)$$

where g is gravitational acceleration, r is the radius of the xenolith, P_x and P_m are the density of the xenolith and magma respectively, and n is the viscosity of the magma. In this case, for a xenolith with a radius of 0.05 m and a density of 2500 kgm^{-3} , within a Ngauruhoe

magma with a viscosity of $\log 3.2 \text{ Pa}\cdot\text{s}$ ($\pm \log 1.5 \text{ Pa}\cdot\text{s}$) or $1800 \text{ Pa}\cdot\text{s}$ and a density of 2400 kgm^{-3} , the settling velocity of a given xenolith is approximately 0.0003 ms^{-1} or 1.0 kmh^{-1} . This velocity must be considered a minimum and it is possible that magma ascent could be significantly faster than this rate. As a comparison, Burgisser & Gardner (2005) suggest that the critical ascent rate at which the style of eruption changes from effusive to explosive behaviour is ca. 0.35 ms^{-1} . Although our calculated ascent rate is significantly slower than their experimental work, there are other factors that are likely to be controlling the style of eruption. Nairn (1976) suggested that the eruption was explosive due to the presence of a substantial amount of water trapped in a cooling magma body at shallow depths. The interaction of the rising magma with the cold groundwater rapidly caused expansion of the water leading to explosive fragmentation.

Complications will arise due to the changing conditions of the magma on ascent, such as crystallisation and cooling (causing an increase in viscosity and potentially slowing xenolith settling) and vesiculation (reducing viscosity). However, this gives a first approximation for the ascent of Ngauruhoe magma in the conduit. According to our fluid inclusion data, the xenoliths are occupying a depth of between 1.5 and 3.5 km for some period of time. If we consider this depth to be a shallow magma chamber/s, the time spent for the magma to ascend in the conduit from that chamber/s, whilst carrying the xenoliths within the fluid is ca. 60 to 130 days or 2 to 4 months. Looking back at the seismic records during the active period of Ngauruhoe between 1973 and 1975 (Latter, 1974; 1975a,b), immediately prior to surface activity, including ash emission or pyroclastic eruption, low-frequency seismicity is present from ca. 2 days to hours before the event. However, there are periods a number of months before surface activity where low frequency events are recorded beneath the cone. These seismic events that occur well before surface activity could represent the first stages of magma migration into the conduit. For the most part, that the lead-in time from the onset of the recorded low-frequency events to eruption was very short and our estimates may be significant underestimates.

During periods of magma replenishment from deeper, hotter and more gas-rich magma batches, it is proposed that the existing storage chambers become gas-charged and begin ascent. The magma rises (probably at greater than our calculated ca. 0.0002 ms^{-1} – up to 0.6 ms^{-1}) and quickly begins to decompress and vesiculate, leading to explosive eruption. During ascent, low-frequency seismicity is produced a matter of months to days before the magma reaches a critical point close to the surface and fragments.

It is possible that during previous events from Ngauruhoe, magma ascent may have been similar to that calculated for the 1975 event (most notably 1954 – 1955), but the amount or availability of water stored in the shallow subsurface could play a more significant role in the style of eruption than first thought. Determining a controlling factor on the differing styles of eruption at Ngauruhoe will be the subject of future work.

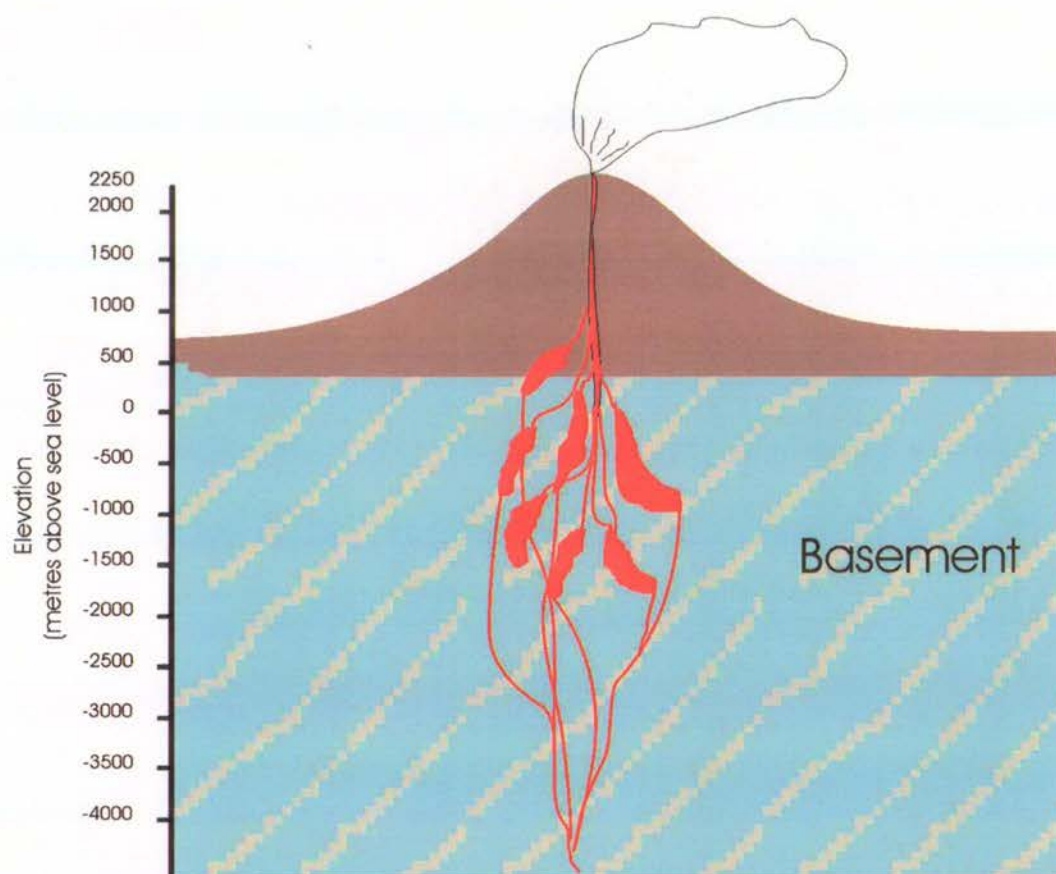


Figure 9 Schematic diagram of the sub-surface magmatic plumbing system determined from this study and Hobden et al. (1999). Note the numerous magma chambers in close proximity but evolving independently.

CONCLUSIONS

We have shown that, through the analysis of fluid inclusions, a potential shallow magma storage zone occurs between 1.5 and 3.5 km depth. This storage zone is likely to be composed of a series of small magma batches that are adjacent to each other, but interaction is limited. At this depth, magma-wall rock interaction is causing the country rock to be incorporated into the magma as xenoliths.

Calculations of magma ascent rate using xenolith settling velocities show that a rate of ca. 0.0002 ms^{-1} must be occurring, thus giving a lead time of potentially a number of months to erupt from the shallow magma chamber. Burgisser and Gardner (2005) note that rapid vesiculation takes place at ascent rates of greater than 0.35 ms^{-1} leading to explosive eruption, thus it is likely that some acceleration or rapid fragmentation may have taken place in the upper conduit prior to the 1975 eruption.

We believe that any future pre-eruptive seismicity may be constrained using our petrological data. The presence of a shallow magma chamber determined through this study, greatly adds to the accuracy of previous estimates that suggested a magma plumbing system with a shallow holding chamber existed at less than 5 km depth. Erosion of the country rock via shearing and fragmentation over a depth interval determined in this study may also be a viable process and our depth control may help to constrain the depth at which seismic events will be produced and recorded in future events.

REFERENCES

- Burgisser, A., Gardner, J.E. 2005. Experimental constraints on degassing and permeability in volcanic conduit flow. *Bulletin of Volcanology* 67:42–56.
- Carmichael, R.S., 1984. *CRC Handbook of physical properties of rocks, Volume III*. CRC Press, Inc. Boca Raton, Florida, USA.
- Clocchiatti, R., Del Moro, A., Gioncada, A., Joron, J.L., Mosbah, M., Pinarelli, L., Sbrana, A. 1994. Assessment of a shallow magmatic system: the 1888-1890 eruption, Vulcano Island, Italy. *Bulletin of Volcanology* 56: 466–486.
- Di Muro, A., Villemant B., Montagnac G., Scaillet B., Reynard B. 2008. Quantification of water content and speciation in natural silicic glasses (phonolite, dacite, rhyolite) by confocal microRaman spectrometry. *Geochimica et Cosmochimica Acta* 70: 2868–2884.
- Giordano, D., Dingwell, D.B. 2003. Non-Arrhenian multicomponent melt viscosity: a model. *Earth and Planetary Science Letters* 208: 337–349.
- Giordano, D., Russel, J.K., Dingwell, D.B. 2008. Viscosity of magmatic liquids: A model. *Earth and Planetary Science Letters* 271: 123–134.
- Graham, I.J. 1987. Petrography and origin of metasedimentary xenoliths in lavas from Tongariro Volcanic Centre. *New Zealand Journal of Geology and Geophysics* 30: 139-157.
- Graham, I.J., Grapes, R.H., Kifle, K. 1988 Buchitic metagreywacke xenoliths from Mount Ngauruhoe, Taupo Volcanic Zone, New Zealand. *Journal of Volcanology and Geothermal Research* 35: 205-216.
- Hobden B.J. 1997 Modelling magmatic trends in time and space: eruptive and magmatic history of Tongariro volcanic complex, New Zealand. PhD Thesis, University of Canterbury, Christchurch
- Hobden BJ, Houghton BF, Davidson JP, Weaver SD (1999) Small and short-lived magma batches at composite volcanoes: time windows at Tongariro volcano, New Zealand. *Journal of the Geological Society of London* 156: 865–868
- Hobden, B.J., Houghton, B.F., Nairn, I.A. 2002. Growth of a young, frequently active composite cone: Ngauruhoe volcano, New Zealand. *Bulletin of Volcanology* 64: 392-409.
- Hui, H., Zhang, Y. 2007. Toward a general viscosity equation for natural anhydrous and hydrous silicate melts. *Geochimica et Cosmochimica Acta*. 71: 403–416.
- Latter, J.J. 1974. Volcanic tremor and B-type earthquakes, Ruapehu and Ngauruhoe in New Zealand Volcanological Record, 1973. New Zealand Geological Survey.
- Latter, J.J. 1975a. Volcanic tremor and B-type earthquakes, Ruapehu and Ngauruhoe in New Zealand Volcanological Record, 1974. New Zealand Geological Survey.
- Latter, J.J. 1975b. Volcanic tremor and B-type earthquakes, Ruapehu and Ngauruhoe in New Zealand Volcanological Record, 1975. New Zealand Geological Survey.
- Latter, J.H. 1981. Volcanic earthquakes, and their relationship to eruptions at Ruapehu and Ngauruhoe volcanoes. *Journal of Volcanology and Geothermal Research* 9: 293-309

- Lima, A. 1996. CO₂ fluid inclusion in a gabbroic xenolith from Panarea (Aeolian Islands): A contribution to the understanding of pressure evolution of the subvolcanic magmatic system. *Acta Vulcanologica* 8: 139–146
- Liu, L-G., Mernagh, T.P. 1990. Phase transitions and Raman spectra of calcite at high pressures and room temperature. *American Mineralogist* 75, 801-806.
- Nairn I.A. 1976. Atmospheric shock waves and condensation clouds from Ngauruhoe explosive eruptions. *Nature* 259:190–192
- Nairn, I.A., Self, S. 1978. Explosive eruptions and pyroclastic avalanches from Ngauruhoe in February 1975. *Journal of Volcanology and Geothermal Research* 3: 39-60
- Rowlands, D. P., White, R. S., Haines, A. J. 2005. Seismic tomography of the Tongariro Volcanic Centre, New Zealand. *Geophysical Journal International* 163: 1180–1194
- Self, S., Wilson, L., and Nairn, I.A., 1979. Vulcanian eruption mechanisms. *Nature* 277: 440–443
- Shaw, H.R. 1972. Viscosities of magmatic silicate liquids: An empirical method of prediction. *American Journal of Science* 272: 870–893.
- Steiner, A. 1958. Petrogenetic implications of the 1954 Ngauruhoe lava and its xenoliths. *New Zealand Journal of Geology and Geophysics* 1: 325-363.
- Vaggelli, G., H. E. Belkin, and L. Francalanci. 1993. Silicate-melt inclusions in the mineral phases of the Stromboli volcanic rocks: A contribution to the understanding of magmatic processes, *Acta Vulcanologica* 3:115–125.
- Zanon, V. Frezzotti, M-L., Peccerillo, A. 2003. Magmatic feeding system and crustal magma accumulation beneath Vulcano Island (Italy): evidence from CO₂ fluid inclusions in quartz xenoliths. *Journal of Geophysical Research* 108 B6, 2298.

ACKNOWLEDGEMENTS

The authors would like to thank Terry Mernagh for his patience and guidance when explaining the intricacies of the Laser Raman at Geoscience Australia. We are also grateful for his help in reducing many of the results into a usable form after the analyses had been completed. Andrew Rae is thanked for his review of this report. This work was made possible through the EQC grant BIE08/553 to GNS Science.



www.gns.cri.nz

Principal Location

1 Fairway Drive
Avalon
Lower Hutt 5010
PO Box 30368
Lower Hutt 5040
New Zealand
T +64-4-570 1444
F +64-4-570 4600

Other Locations

Dunedin Research Centre
764 Cumberland Street
Dunedin 9016
Private Bag 1930
Dunedin 9054
New Zealand
T +64-3-477 4050
F +64-3-477 5232

Wairakei Research Centre
114 Karetoto Road, Wairakei
Taupo 3377
Private Bag 2000
Taupo 3352
New Zealand
T +64-7-374 8211
F +64-7-374 8199

National Isotope Centre
30 Gracefield Road, Gracefield
Lower Hutt 5010
PO Box 31312
Lower Hutt 5040
New Zealand
T +64-4-570 1444
F +64-4-570 4657